FISCHER-TROPSCH SLURRY PHASE PROCESS VARIATIONS TO UNDERSTAND WAX FORMATION: QUARTERLY REPORT FOR PERIOD JULY 1, 1988 TO SEPTEMBER 30, 1988

MASSACHUSETTS INST. OF TECH., CAMBRIDGE

1988

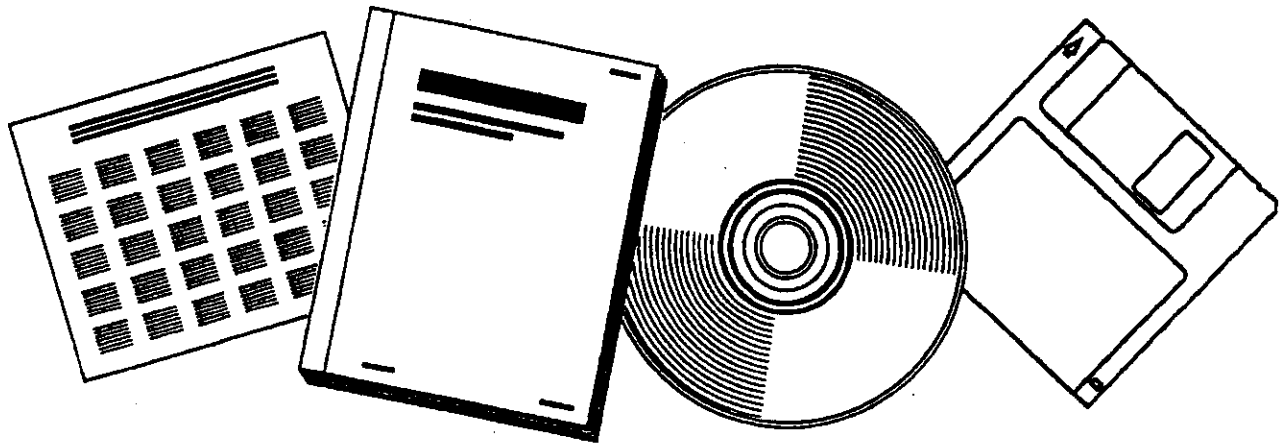

U.S. DEPARTMENT OF COMMERCE
National Technical Information Service

DOE/PC/80015--12

DE89 003247

Fischer-Tropsch Slurry Phase Process Variations to Understand Wax Formation

Quarterly Report for Period

July 1, 1988 to September 30, 1988

Report No.: DOE/PC80015-12

Contract No.: DE-AC22-85PC80015

by

Timothy Donnelly and

Charles N. Satterfield

for

U.S. Department of Energy

Pittsburgh Energy Technology Center

P.O. Box 10940-MS 902-L

Pittsburgh, PA 15236

Attention: William E. McKinstry, Project Manager

NOTICE

This report was prepared as an account of work sponsored by an agency of the United States Government. Neither the United States nor any agency thereof, nor any of their employees, makes any warranty, expressed or implied or assumes any legal liability or responsibility for any third party's use or the results of such use of any information, apparatus, product or process disclosed in this report, or represents that its use by such third party would not infringe privately owned rights.

Summary

A precipitated iron catalyst without any alkali promoters was studied for 2000 hours on stream in a slurry reactor. Reaction conditions were 230 to 260°C (mostly 260°C), 0.77 to 1.92 MPa, H_2/CO feed ratios of 0.5 to 2.0 and $CO + H_2$ conversions of 10% to 65%. A Schulz-Flory carbon number distribution with two chain growth probabilities was required to describe the products. Effects of operating variables on 1-butene/n-butane ratio, methane and oxygenate selectivities, and α_1 and α_2 are reported. Kinetic models for secondary reactions of 1-alkenes were developed. Addition of potassium t-butoxide to the reactor substantially shifted both distributions to heavier products.

INTRODUCTION

All iron Fischer-Tropsch catalysts that have been used industrially contain potassium, in part because potassium helps to stabilize the catalyst against aging. Little information has been published about the performance characteristics of iron catalysts without alkali under representative industrial conditions. However this is needed to help clarify the role of potassium.

Alkalized iron catalysts require two chain-growth parameters in a Schulz-Flory distribution to describe the product (1,2,3,4,5). This is sometimes termed a "double-α" distribution, and suggests that two kinds of mechanisms are involved. Schliebs and Gaube (2) have hypothesized that one type of catalyst site contains potassium and the second is without potassium, and they have presented some experimental data in support of this position. Particularly they report that an unalkalized catalyst requires only a single chain growth probability, α. To the contrary, we find clear evidence that a double-α distribution occurs even in the absence of potassium, as will be shown.

Information is also presented on the effects of operating parameters on the selectivity of this catalyst to 1- and 2-alkenes, methane, and oxygenates.

EXPERIMENTAL

Composition

The precipitated iron catalyst was prepared by the Pittsburgh Energy Technology Center (PETC), under the supervision of M.F. Zarochak. Catalyst precursor batches were prepared in a

continuous stirred precipitation reactor. Iron and copper were co-precipitated from a nitrate solution with ammonium hydroxide. The filter cake, about 100 grams, was washed with 8 liters of hot deionized water, then dried under flowing nitrogen for 24 hours at 110°C and under vacuum for 24 hours at 110°C. A summary of the procedure is given by Zarochak, et al. (6).

The catalyst was analyzed by Galbraith Laboratories for iron, copper, silica, potassium, and sodium. Table 1 gives the composition as determined by atomic absorption spectroscopy. No potassium or sodium was detected at the minimum measurable limits of 8 ppm and 12 ppm, respectively. The catalyst does not contain silica.

Pretreatment

The catalyst was ground and sieved to 50 to 90 μm (170 to 270 ASTM mesh) and calcined in air at 130°C for 24 hours prior to pretreatment. This reduced the catalyst weight by 10.1 wt%. 26.8 grams of calcined catalyst were charged to the 1 liter slurry reactor and the reactor system was then sealed and leak-tested with helium to 2.13 MPa.

The catalyst was pretreated according to a procedure described by Zarochak, et al. The reactor temperature was brought to 280 °C while the catalyst and slurry liquid were held under helium at 1.48 MPa. Then CO was introduced at 0.02 Nl/min/gcat for 24 hours. This procedure reportedly gives improved selectivity to heavy products and more stable activity than pretreatment under 1:1 H_2/CO at the same flow rate.

Reactor Conditions

The slurry reactor and methods of operation are described elsewhere (7,8). The reactor was first charged with 400 grams of n-octacosane (Humphrey). The octacosane had been recrystallized in tetrahydrofuran (THF) to remove a bromine impurity that is introduced during the synthesis by coupling of bromotetradecane.

The reactor was fed from a dual manifold system with Brooks 5850 mass flow meters and a Brooks 5878 controller maintaining H_2 and CO flow. Whenever the reactor was taken off-stream for more than 30 minutes, the reactor and traps were vented, then flushed and repressurized with helium.

Material balances were carried out for 6 to 24 hours, with at least 10 hours allowed between material balances to ensure steady state operation. When the reactor temperature or pressure was varied, at least 30 hours were allowed between material balances. Products were collected in two traps, one kept at 80°C and the other at 3°C. Non-condensable gases continued past a sampling valve to an on-line gas chromatograph, then were vented after passing through soap bubble meters.

Material balances based on overhead products closed to within $\pm$ 5% on oxygen. Some carbon and hydrogen remain as waxy products in the reactor, so closures for those elements are generally lower than for oxygen (9). Good product distributions are often obtained, even when carbon and hydrogen closure is poor. This is because most of the gas fed to the reactor also leaves the reactor as non-condensable gas (ie. CO, H_2, CO_2). Only the hydrocarbon and oxygenated organic products of the synthesis are generally of interest. The hydrocarbon products

consist primarily of n-alkanes and 1- and 2-alkenes. Smaller quantites of other hydrocarbons, mostly methyl-branched alkanes are also formed. In presenting carbon-number distributions, all components are lumped together at each carbon number. In discussing 1-olefin/paraffin ratios only the normal species are included.

Reactor temperature was varied between 230 and 260°C, with most experiments at 260°C. Pressures were varied from 0.77 to 1.92 MPa and H_2/CO feed ratios from 0.5 to 2.0. Conversions were varied from 10 to 65% by changing space velocity between 0.010 and 0.040 Nl/min/gcat. These conditions allow for comparison with experiments reported by PETC on a potassium-promoted batch of this catalyst and with our studies on a precipitated iron catalyst containing potassium discussed elsewhere (10).

Products were analyzed by use of three gas chromatographs, as described by Huff, et al. (11). A Hewlett-Packard 5880 with a dimethyl silicone capillary column and a flame ionization detector (FID) was used for hydrocarbon analyses, and for organic liquid samples from the hot and cold traps. Water and oxygenated hydrocarbons and aqueous liquid samples from the hot and cold traps were analyzed with a Hewlett-Packard 5710 using a Tenax packed column and a thermal conductivity detector (TCD). A Carle Refinery Gas Analyzer (RGA) was used exclusively for the analysis of non-condensable gases, particularly CO, H_2, and CO_2. Non-condensable gases were also determined with the other two systems. Tie components, CO_2, CH_4, and C_2 and C_3 compounds, were used to match the analyses from the three GC's and provide a

complete product distribution.

The RGA uses a series of packed columns and a switching valve to separate CH_4, C_2 and C_3 compounds, CO, and CO_2. H_2 separation is accomplished by a hydrogen transfer system (HTS), which is a hydrogen-permeable palladium thimble. This system uses N_2 as a carrier, while all other separations in all three GCs use helium. The HTS avoids the problems associated with the similar responses of He and H_2 in a TCD.

Catalyst activity declined significantly during the 2000 hours it was on stream; however, selectivity did not seem to change with time. Wax samples were drawn from the reactor periodically to determine the carbon number distribution of non-volatile products. After 1400 hours potassium t-butoxide was added to the reactor and a limited amount of data was obtained on its effect.

RESULTS AND DISCUSSION

Carbon Number Distribution

Twenty-eight usable material balances were obtained on the unalkalized catalyst, followed by five obtained after the addition of potassium t-butoxide. For all material balances, the total hydrocarbon products at each carbon number follow a Schulz-Flory distribution with two chain growth parameters, α_1 and α_2. These were calculated using the non-linear least squares regression, described by Donnelly, et al. (12).

Figure 1 shows carbon number distributions for four experiments, all at 260°C, 1.48 MPa, and 0.02 Nl/min/gcat of 1:1 H_2/CO flow, taken at different times-on-stream.

While data at low carbon numbers are very consistent, mole fractions at high carbon numbers on an absolute basis are less so because of experimental problems. Small increases and decreases from run to run typically occur near about C_9 because of slight errors in the weights of liquid products collected in the traps. If a small amount of liquid is lost by "splatter", then the mole fractions of heavy products appear artificially low. Similarly, the hot organic phase solidifies quickly at room temperature, and small amounts of the aqueous phase are sometimes entrapped in the wax. This can cause a slight increase in the apparent mole fractions of heavy products. This problem is intensified in the present studies by the low activity of this particular catalyst and the low catalyst loading, which result in low yields of liquid products. However the slopes on the Schulz-Flory plot a few carbon numbers higher than C_9 are repeatable. The values of α_2 calculated from the non-linear least squares regression were determined by excluding any individual points which fell too far from the curve.

Figure 2 is a Schulz-Flory diagram of a wax sample taken after the first 170 hours-on-stream, kept constant at 260°C and 0.037 Nl/(min)(gcat) of 1:1 H_2/CO flow. Figure 3 is a Schulz-Flory diagram of volatile hydrocarbon and oxygenated hydrocarbon products from a material balance under the same conditions at a time-on-stream of 665 hours. The curve is fitted by non-linear regression. The value of α_2 calculated by the non-linear regression of the volatile sample agrees with that calculated by linear regression of the wax sample, and is equal to 0.88.

Schliebs and Gaube (2) and Konig and Gaube (3) have reported that, in the absence of alkali promoters, the hydrocarbon products of the Fischer-Tropsch synthesis on precipitated iron catalysts can be described by a single-α. We do not find this to be the case. Atomic absorption spectroscopy by Galbraith Laboratories on two samples of this catalyst detected no potassium or sodium at the measurable limits of 9 and 12 ppm. Dictor and Bell (5) and Itoh, et al. (13) have also reported that products from unalkalized Fe_2O_3 powders could not be described well by a single-α. Re-analysis of data from Schliebs's thesis (14) by Donnelly, et al. (12) shows that the data reported by Schliebs and Gaube (2) are not representative of typical experiments. In fact, all of the data collected by Schliebs on potassium-promoted and potassium-free precipitated iron require two values of α to be fit properly, as discussed (12).

The effects of operating variables on α_1, calculated by linear regression of C_3 to C_7 data and α_2, calculated by the non-linear regression are summarized below. The previously reported study that most closely resembles ours, both with respect to carbon-number distribution and specific products, is that by Dictor and Bell (5). However they do not explicitly discuss effects of operating variables on α_2. The catalysts discussed in this and a previous report were precipitated iron catalysts prepared by PETC and Ruhrchemie. This latter contains potassium and silica and is representative of low temperature iron catalysts used at SASOL. Dictor and Bell used low surface area Fe_2O_3 powders (Alfa Products). For several of their experiments,

they added about 0.6 wt% potassium to the iron oxide by immersing the Fe_2O_3 powder in a K_2CO_3 solution. In general their catalysts, with and without potassium, behaved similarly to our analogous catalysts, as will be shown.

The two laboratories use similar slurry reactors and trapping systems. The carrier used in our experiments was recrystallized n-octacosane, which is easily identified on gas chromatograms. Dictor and Bell used Amoco Parowax, which is a mixture of C_{20} to C_{45} paraffins with traces of C_{16} to C_{19} paraffins. Their useful data, therefore, were limited to fairly volatile products; there may have been some carryover of the lighter fraction of the slurry into their volatile fraction. For their unalkalized Fe_2O_3 powders, they used relatively low temperatures of reaction, 188 to 241°C, possibly to minimize volatilization from the original pot liquid. Our studies were primarily at 260°C, which affords comparison with other data in the literature. CO conversion for their experiments was kept below 5%, while our experiments here were carried out between 10 and 65% conversion.

Temperature: Only five experiments were carried out at temperatures other than 260°C, so our conclusions regarding temperature dependence are limited. Figure 4 shows that over the range 232 to 260°C, α_1 is about 0.65 and α_2 about 0.90. In experiments with considerably more data at different temperatures the potassium-promoted Ruhrchemie catalyst showed a decrease of α_1 with increased temperature, with α_2 remaining constant at about 0.90 (10). Dictor and Bell reported a decrease in α_1 from

0.68 to 0.59 on potassium-free Fe_2O_3 powders as temperature was increased from 188 to 241°C.

Conversion: Both α_1 and α_2 were relatively insensitive to conversion over the range of 8 to 61%. We likewise saw no effect of conversion with the Ruhrchemie catalyst and Dictor and Bell report comparable results.

H_2/CO Ratio: Figure 5 shows little effect of H_2/CO ratio in the reactor on the values of α_1 and α_2 over the H_2/CO range studied from 0.3 to 3. This agrees with results given by Dictor and Bell, using potassium-promoted and potassium-free Fe_2O_3 powders, and by Schliebs and Gaube (2), using precipitated iron catalysts. Matsumoto (7) has reported a decrease in α_1 at very high H_2/CO ratios on a fused magnetite catalyst, but these ratios were not studied here.

Component Schulz-Flory Diagram

Figure 6 is a Schulz-Flory diagram showing the distribution of several product classes for a material balance at 260°C, 1.38 MPa, and 0.02 Nl/(min)(gcat) of 1:1 H_2/CO flow.

A double-α is shown for n-alkanes and 1-alkenes, although that for 1-alkenes becomes more obvious on addition of potassium, as shown on Figure 7, discussed below. 2-alkenes are fit reasonably well by a single-α; however, only C_4 through C_{12} 2-alkenes can be resolved by our gas chromatographic techniques. With increasing carbon number, concentrations drop steadily and the G.C. peaks for the 1- and 2-alkenes and the n-alkane become squeezed together. It is possible some of the 2-alkenes present at high carbon numbers are included in the n-alkane peak, so it

may be that a double-α is required to describe 2-alkene distributions. Similarly, the analysis for 1-alkenes may give artificially low concentrations at high carbon numbers. This means that values reported for α_2 for 1-alkenes may also be too low. The only oxygenate detected was methanol, in contrast to the behavior of catalysts containing potassium.

Secondary reactions, such as 1-alkene isomerization and hydrogenation (see below) also occur, so the 1-alkene/n-alkane ratios in Figure 6 are determined by the particular operating conditions studied. Egiebor, et al. (4) and Wojciechowski (15) have interpreted component Schulz-Flory diagrams such as this by erroneously ascribing all products to a primary set of reactions. Reaction networks developed on this assumption can be misleading.

Addition of Potassium

After 1400 hours-on-stream, 0.7 g. of potassium t-butoxide was added to the reactor under helium. If this all adsorbed onto the catalyst, it would be equivalent to 1.0 wt% K on an unreduced catalyst basis. The reactor was then operated with a 1:1 H_2/CO flow at 0.02 Nl/(min)(gcat) at 260°C and 1.48 MPa for 72 hours before additional material balances were made. By 1400 hours on stream the catalyst activity had decreased substantially and concentrations of some minor products could not be determined reliably.

Figure 8 is a Schulz-Flory diagram comparing experiments at identical process conditions, before and after the addition of the potassium. α_1 increased from 0.64 to 0.68 and α_2 increased from 0.88 to 0.94. The increase in α_2 is particularly important

in increasing selectivity to heavy products. Table 2 shows the weight percent of products in several important carbon number ranges before and after potassium addition. The diesel fuel and wax fractions increase markedly.

Figure 7 is a Schulz-Flory diagram of component classes after potassium addition. Virtually no olefin isomerization occurs. Oxygenates from C_1 to C_6 are formed in slightly greater quantity than on the unalkalized catalyst and they are described well by a single-α. In contrast on the unalkalized catalyst only methanol was detected.

Comparison With Other Catalysts

Prior to potassium addition, products collected over the unalkalized catalyst followed a distribution similar to those using the United Catalysts C-73 fused iron catalyst. After potassium addition, the products from this catalyst followed a similar distribution to products from the alkalized PETC catalyst used by Zarochak, et al. (6), the Mobil low-wax catalyst reported on by Kuo (16), and the Ruhrchemie catalyst studied in this laboratory. These comparisons are discussed in more detail elsewhere (10).

RESULTS - OLEFIN HYDROGENATION

The principal type of hydrocarbon formed by the primary synthesis is the 1-alkene. This then may be hydrogenated to a n-alkane or isomerized to the 2-alkene. The effects of temperature, conversion and H_2/CO ratio on these two secondary reactions were studied by focussing on C_4 products. These exist only in the vapor phase at room temperature, thus eliminating

possible problems with splitting of products between vapor and liquid phases in traps. The ratio of 1-butene/n-butane varied over the range 1.0 to 6.0, dependent predominantly on the pressure of hydrogen in the reactor.

Temperature: With constant H_2/CO ratio in the feed, the 1-alkene/n-alkane ratio was relatively independent of temperature, based on limited data. After potassium addition, the catalyst showed an increase in this ratio from about 2.5 to 3.7 as temperature was increased from 232 to 260°C.

On potassium-free Fe_2O_3 powders, Dictor and Bell report a decrease in alkene/alkane ratio with increased temperature. When potassium was present, they observed an increase, as we did here and with the Ruhrchemie catalyst. Schulz, Rosch, and Gokcebay (17) report the opposite; that alkalized iron catalysts showed an increased selectivity to alkanes as temperature was increased from 220 to 280°C. The reasons for this difference are not clear.

Conversion: The ratio of 1-butene to n-butane was independent of space velocity and similar behavior was observed using the Ruhrchemie catalyst. After potassium addition, a slight increase in selectivity to 1-butene with increasing space velocity was observed. Dictor and Bell have reported a slight increase in olefin content with increased space velocity on potassium-free Fe_2O_3 powders at high H_2/CO ratios. Arakawa and Bell (18) have also reported an increase in 1-alkene/n-alkane ratio with increased space velocity on alumina supported potassium-promoted and potassium-free iron catalysts. However, they saw this effect

only at space velocities nearly ten times as great as those used in the current experiments and corresponding CO conversions of about 5%. For their experiments at space velocities and conversions comparable to ours, they show no effect of space velocity on 1-alkene/n-alkane ratio.

Effect of H_2/CO in Reactor: Figure 9 shows that the ratio of 1-butene to n-butane sharply decreased from near 6 to about 1 as H_2/CO was increased from 0.3 to 3. Dictor and Bell, using a differential reactor, have reported that alkene/alkane ratio decreases with increasing H_2 pressure, but is relatively insensitive to CO pressure. In contrast, Sudheimer and Gaube (18) have reported that the 1-alkene content increases with increasing CO pressure, but is relatively insensitive to H_2 pressure.

Our data indicate that olefin selectivity increases with both increased CO pressure and decreased H_2 pressure, varied independently. Each of these pressures was varied over the range 0.3 to 1.1 MPa.

Effect of Potassium: Figure 10 shows the dependence of 1-alkene/n-alkane on carbon number for experiments before and after the addition of potassium t-butoxide. Potassium promotion increased 1-alkene/n-alkane ratios strongly, particularly at high carbon numbers. In both the presence and absence of potassium, the ratio decreases with increased carbon number, as has been shown in various other studies. Dictor and Bell likewise reported that selectivity to 1-alkenes was considerably greater in the presence of potassium.

Kinetic Modelling of 1-Butene Hydrogenation

A large number of experimental studies now show that on iron catalysts at elevated pressures the principal hydrocarbon formed by the primary synthesis is a 1-alkene. Paraffins may also be formed by the primary synthesis, but to a much lesser extent. Hydrogenation of alkenes to alkanes is a significant reaction the extent of which varies with catalyst composition, especially potassium content, and reaction conditions. 1-alkenes are readily hydrogenated, but 2-alkenes, which are formed by secondary isomerization, are much less readily hydrogenated, as shown by Sudheimer and Gaube (19). Hydrogenation rates increase with decreased CO concentration, as usually occurs at high conversion.

Sudheimer and Gaube report a study at 0.5 to 1.7 MPa and 220°C of Fischer-Tropsch synthesis on a precipitated iron catalyst containing potassium, but without silica. Their study focused on the fate of the unbranched 1-alkenes formed. Hydrogenation of a particular 1-alkene was inhibited by CO, but also by adsorption of other 1-alkenes, as they showed by adding 1-decene to the system.

A simple expression for the rate of hydrogenation of an adsorbed olefin, say 1-butene, can be written by assuming the rate to be proportional to hydrogen pressure and to the fraction of the surface sites covered with adsorbed 1-butene:

$$R_{butane} = k P_{H2} \theta_{1\text{-butene}} \qquad (1)$$

Assuming complete coverage of all sites and competitive adsorption with CO and other 1-alkenes taken as a group, (C_2 to

C_{3o}), $\theta_{1\text{-butene}}$ can be written:

$$\theta_{1\text{-butene}} = \frac{K_{1\text{-butene}}\, P_{1\text{-butene}}}{K_{CO}\, P_{CO} + K_{1\text{-alkenes}}\, P_{1\text{-alkenes}}} \qquad (2)$$

where Ks are temperature dependent adsorption coefficients. Substituting equation (2) into equation (1) and rearranging:

$$\frac{P_{H2}\, P_{1\text{-butene}}}{P_{1\text{-alkenes}}\, R_{butane}} = \frac{K_{CO}}{k\, K_{1\text{-butene}}} \times \frac{P_{CO}}{P_{1\text{-alkenes}}} + \frac{K_{1\text{-alkenes}}}{k} \qquad (3)$$

Sudheimer and Gaube (18) have developed a similar model, but with adjustable orders of reaction. Equation (3) implies a linear relationship for data obtained at a single temperature, with the intercept depending only on the relative values of an adsorption constant and a rate coefficient.

Figure 11 is a plot at 260°C of the left-hand side of Eq. 3 versus $P_{CO}/P_{1\text{-alkenes}}$. For conversions below 40%, this hydrogenation model appears to fit the data well. At higher conversions some other unknown factor is involved. Simpler models excluding either CO or olefin inhibition do not fit the data well.

Figure 12 is a plot of butane formation rate divided by hydrogen pressure versus 1-butene pressure for several space velocities. The zero intercept suggests that for this set of circumstances essentially all n-butane was formed by secondary hydrogenation.

Isomerization

The isomerization activity of this catalyst is significantly greater than that of catalysts containing potassium. This is shown, for example, by comparison with the studies in our

accompanying paper (10). This effect was also reported by Sudheimer and Gaube and Dictor and Bell. The ratio of 2-butene to 1-butene varied from zero to one, dependent both on gas composition and temperature. The addition of potassium t-butoxide to the reactor suppressed almost all isomerization.

Temperature: Figure 13 shows that the ratio of 2-butene to 1-butene, at a fixed H_2/CO ratio, increases somewhat as temperature is increased. Matsumoto (7) has reported a similar trend on the C-73 fused iron catalyst over the range 232 to 310°C. Dictor and Bell have reported that the ratio of 2-alkene to 1-alkene produced on potassium-free Fe_2O_3 powders increases slightly as temperature increases. Schulz, Rosch, and Gokcebay (16) have reported the same effect for promoted iron catalysts.

Effect of H_2/CO: The isomerization of 1-butene to 2-butene increases with the H_2/CO ratio in situ, as shown in Figure 14. Dictor and Bell report similar results. The opposite effect was reported by Matsumoto (7), for a fused magnetite catalyst containing potassium. In his work, as the H_2/CO ratio at the inlet was increased from 0.7 to 3.8, the ratio of 2-alkene/1-alkene decreased from 0.13 to 0.06 at 310°C.

Kinetic Modelling of 1-Butene Isomerization

For a simple model, we postulate that 2-alkenes are produced by a simple first-order irreversible reaction. The rate can then be expressed as:

$$R_{2\text{-butene}} = k\,\theta_{1\text{-butene}} \qquad (4)$$

Here, k is a temperature-dependent rate constant. If we allow for inhibition by 1-alkenes and carbon monoxide, $\theta_{1\text{-butene}}$ can be

expressed by Eq. 2 as before. Substituting and rearranging:

$$\frac{P_{1\text{-butene}}}{P_{1\text{-alkenes}}\, R_{2\text{-butene}}} = \frac{K_{CO}}{k\, K_{1\text{-butene}}} \times \frac{P_{CO}}{P_{1\text{-alkenes}}} + \frac{K_{1\text{-alkenes}}}{k\, K_{1\text{-butene}}} \quad (5)$$

The model can be tested by plotting the left-hand side of Eq. 5 versus $P_{CO}/P_{1\text{-alkenes}}$.

Figure 15 shows that data from experiments at 260°C are well fitted by this model. This suggests that, at high conversions, competitive adsorption by 1-alkenes makes their inhibiting effects more important relative to CO.

Other Products

The methanation selectivity of this catalyst is high, presumably because of the lack of potassium. The percent of total products as methane varied from about 16 to 44 wt%, and showed some dependence on gas composition, but very little dependence on temperature, space velocity, or H_2 pressure. Figure 16 shows that the mole fraction of products as methane decreased approximately linearly with increasing CO pressure.

Kinetic modelling of methane formation rate was inconclusive. Dictor and Bell have shown a first-order dependence of methane production rate on hydrogen pressure at fixed CO pressure for a potassium-free Fe_2O_3 powder.

Oxygenates generally constituted 4 to 12 wt% of the products, but no significant variation of temperature, space velocity, H_2/CO ratio, or time-on-stream was found.

Effect of Time-on-Stream

This catalyst deactivated rapidly for the first 100 hours-on-stream, then continued to deactivate at a slower rate

throughout the run, as shown in Figure 17. This reinforces comments in the earlier literature to the effect that one of the reasons for adding potassium to an iron catalyst is to help stabilize it against aging. Occasional runs at low reactor H_2/CO, about 0.3, appeared to reversibly re-activate the catalyst. This effect was discovered late in the run and no further study of this effect was made.

References

1. Huff, G.A. and Satterfield, C.N., J. Cat., 85, 370 (1984).

2. Schliebs, B. and Gaube, J., Ber. Bunsenges. Phys. Chem., 89, 68 (1985).

3. Konig, L. and Gaube, J., Chem.-Ing. Tech., 55, 14 (1983).

4. Egiebor, N.O., Cooper, W.C., and Wojciechowski, B.W., Can. J. Chem. Eng., 63, 826 (1985).

5. Dictor, R.A. and A.T. Bell, J. Cat., 97, 121 (1986).

6. Zarochak, M.F., M.A. McDonald, and V.U.S. Rao, "Stability and Selectivity of Potassium Promoted Iron Catalyst in Slurry Fischer-Tropsch Synthesis", 12th Annual Conference on Fuel Sciences, Palo Alto, May 13-14, 1987. Also private communication from Zarochak (1985).

7. Matsumoto, D.K., Effects of Selected Process Variables on Performance of an Iron Fischer-Tropsch Catalyst, Sc. D. thesis, Massachusetts Institute of Technology (1987).

8. Huff, G.A. and C.N. Satterfield, Ind. Eng. Chem. Fund., 21, 479 (1982).

9. Huff, G.A., Fischer-Tropsch Synthesis in a Slurry Reactor, Sc.D. thesis, Massachusetts Institute of Technology (1982).

10. Donnelly, T.J. and C.N. Satterfield, Appl. Catal., submitted.

11. Huff, G.A., C.N. Satterfield, and M.H. Wolf, Ind. Eng. Chem. Fund., 22, 258 (1983).

12. Donnelly, T.J., I.C. Yates, and C.N. Satterfield, (in press).

13. Itoh, H., H. Hosaka, T. Ono, and E. Kikuchi, Appl. Catal., 40, 53 (1988).

14. Schliebs, B., Untersuchungen zur Selktivitat der Fischer-Tropsch-Synthese an Eisenkatalysatoren, Dr.-Ing. dissertation, Technischen Hochschule Darmstadt (1983).

15. Wojciechowski, B.W., Can. J. Chem. Eng., 64, 149 (1986).

16. Kuo, J.C.W., Slurry Fischer-Tropsch/Mobil Two-Stage Process of Converting Syngas to High Octane Gasoline, Final Report, DOE/PC/30022-10 (DE84004411), 1983.

17. Schulz, H., Rosch, S., and Gokcebay, H., Proc. 64th CIC Coal Symp., (A.M. Al Taweel, Ed.), Ottowa (1982).

18. Arakawa, H. and Bell, A.T., Ind. Eng. Chem. Proc. Des. Dev., 22, 97 (1983).

19. Sudheimer, G. and J. Gaube, Ger. Chem. Eng., 8, 195 (1985).

Table 1

Composition of Precipitated Iron Catalyst

Fe	60.46 wt%
Cu	0.58
SiO_2	< 0.002
K	< 9 ppm
Na	< 12 ppm
O	38.96

All compositions determined by duplicate analysis using atomic absorption spectroscopy by Galbraith Laboratories, except oxygen by difference. Oxygen is assumed to be bound as metallic oxides.

Table 2
Effect of Potassium on Product Cuts

	No Potassium	1 wt% Potassium
C_1	10.2 wt%	5.3 wt%
C_2-C_4	32.4	23.1
C_5-C_{12}	39.8	34.1
$C_{13}-C_{19}$	11.7	20.6
C_{20+}	5.9	16.9

Table 3

Summary of Selectivity Information

Legend

MB	Material balance number
T	Temperature, °C
Qo	Inlet flow rate, Nl/min
Clos.	Wt. % closure on oxygen
H_2/CO	Reactor H_2/CO ratio
CH_4 mol %	Mole % of methane in hydrocarbon and oxygenated products
Oxy. wt %	Weight % of oxygenates (aldehydes + ketones + alcohols) in products
alp 1 lin reg	α_1 calculated by linear regression of C_3 to C_7 hydrocarbon plus oxygenated products
Non-linear regr. alp 1 and alp.2	α_1 and α_2 calculated by non-linear least squares regression of hydrocarbon plus oxygenated products

Note: Complete information is not available for all material balances. Material balances 37 to 40 were performed after catalyst activity had become very low, so very little liquid product was collected, making complete material balances difficult. Material balances 30 through 33 were affected by flow and trapping problems. Complete material balances for material balances 25 and 26 will be available after further chromatographic analyses.

ID	°T deg C	Gr Nl/min	Clos. % ovr	% conv CO+H2	H2/CO	1-butene n-butane	2-butene 1-butene	CH4 mol %	Oxy. wt %	alp 1 lin reg	Non-linear regr. alp 1	alp 2
1	260	0.510	75.[illegible]	60.6	0.56	2.5[illegible]	0.43	26.5	4.9	0.63	0.62	0.90
2	260	1.559	99.7	21.2	0.94	2.72	0.40	32.9	7.2	0.65		
3	260	1.052	96.5	30.1	0.91	2.66	0.44	31.5	7.6	0.63	0.55	0.55
4	260	1.046	101.0	23.4	0.55	3.85	0.29	31.3	3.5	0.65	0.57	0.92
5	260	1.026	105.2	16.9	0.35	5.55	0.15	23.3	7.2	0.69	0.67	0.59
6	260	1.060	91.4	36.3	2.95	1.05	0.93	37.2	6.9	0.62	0.55	0.59
7	260	1.056	97.4	31.5	0.57	2.60	0.35	26.0	7.9	0.67	0.62	0.50
8	260	1.037	101.2	25.0	0.86	2.65	0.36	21.7	7.0	0.64	0.61	0.50
9	260	1.020	101.0	14.4	1.02	2.63	0.61	35.1	10.3	0.64	0.54	0.79
10	260	0.950	102.4	14.1	0.97	2.64	0.62	29.9	6.2	0.67	0.64	0.91
11	260	1.039	101.7	23.1	0.90	2.65	0.44	31.1	6.5	0.69	0.64	0.55
12	260	0.465	55.7	45.6	0.57	2.53	0.46	25.7	5.6		0.51	0.57
13	260	0.442	51.0	44.5	0.55	2.52	0.46	26.6	4.2	0.65	0.66	0.55
14	260	1.325	95.2	15.5	0.95	2.75	0.36	25.5	9.2	0.67	0.69	0.56
15	260	1.119	92.1	23.2	0.37	5.46	0.17	19.7	11.0	0.67	0.62	0.93
16	260	1.060	91.7	32.7	2.74	1.11	0.92	35.4	5.5	0.61	0.60	0.55
17	260	1.049	97.5	15.3	0.40	5.09	0.20	23.5	9.1	0.65	0.65	0.65
18	260	0.962	105.4	15.4	0.92	2.60	0.44	17.0	15.1	0.66		
19	260	1.095	59.7	30.2	0.94	2.54	0.43			[illegible]	0.57	0.93
20	[illegible]	1.074	96.0	5.5	1.00	2.94	0.00	33.0	11.4	0.61	0.60	0.57
21	232	1.054	94.5	10.2	1.01	2.80	[illegible]	25.7	15.5	0.66	0.77	0.93
22	245	1.073	92.6	16.1	1.00	2.32	0.20	30.9	19.1	0.62	0.61	0.93
23	245	1.200	53.4	22.9	1.00	2.17	0.19	31.5	14.5	0.65	0.58	0.59
24	245					2.15	0.20	32.1		0.63		
25	260											
26	260											
27	260	0.953	100.7	15.0	0.39	4.47	0.15	30.5	7.5	0.70	0.64	0.90
28												
29	260	0.940	55.9	26.5	2.76	0.76	0.59	44.0	10.2	0.61	0.56	0.91
30												
31												
32												
33												
34	260	0.815	100.1	17.2	0.68	3.84	0.00			0.72		
35	260	0.809	99.3	14.9	0.70	3.57	0.00	23.9	4.5	0.72	0.68	0.94
36	260	0.460	95.1	22.9	0.70	3.46	0.00			0.70		
37												
38	232	0.799	95.2	4.0	0.70	2.59	0.00					
39	232	0.799	100.6	2.1	0.69	2.55	0.00					
40	260	0.934	105.0	6.7	0.41	3.79	0.00					

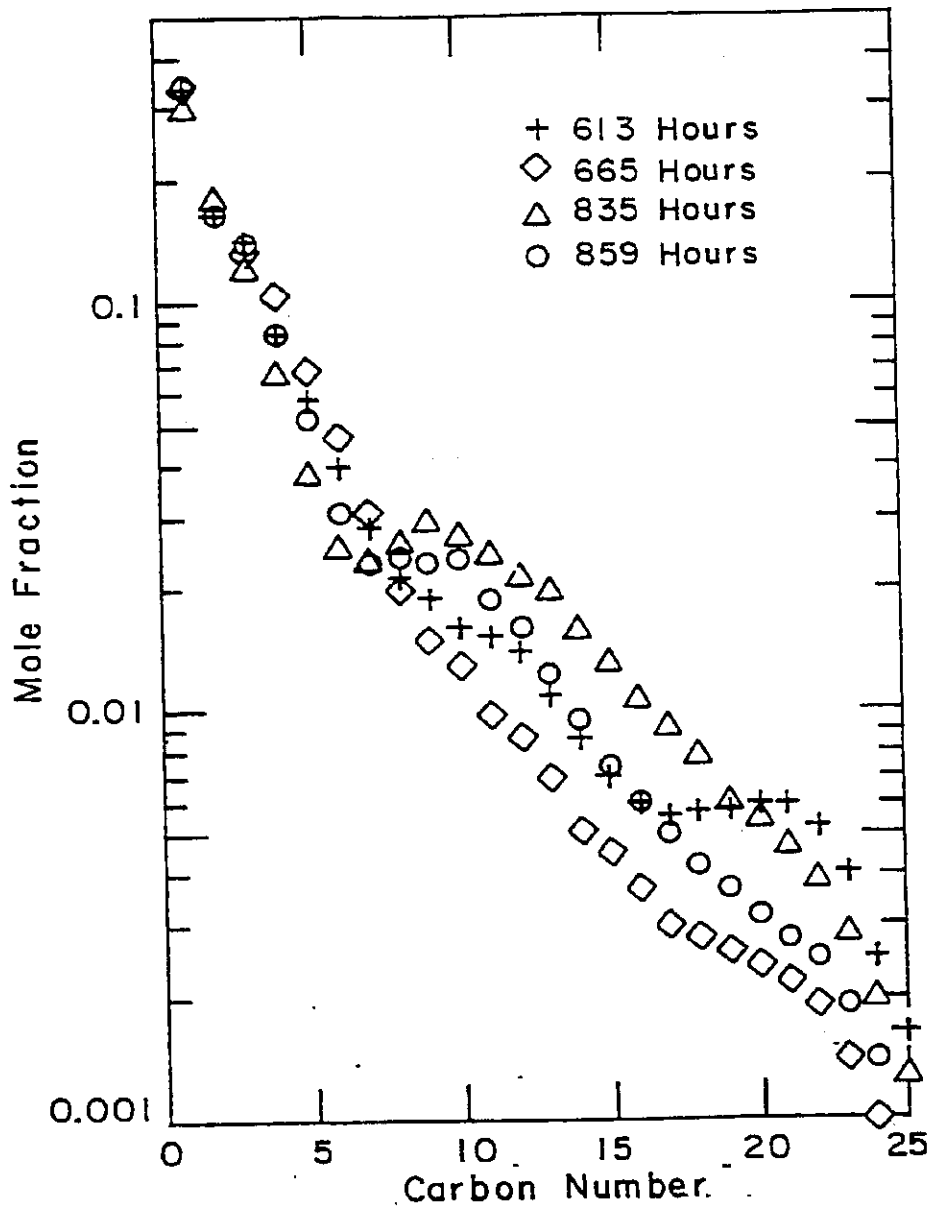

Figure 1 Comparative Schulz-Flory Diagrams for Material Balances at four different times on stream. 260°C, 1.48 MPa, 0.022 Nl/min/gcat 1:1 H_2/CO.

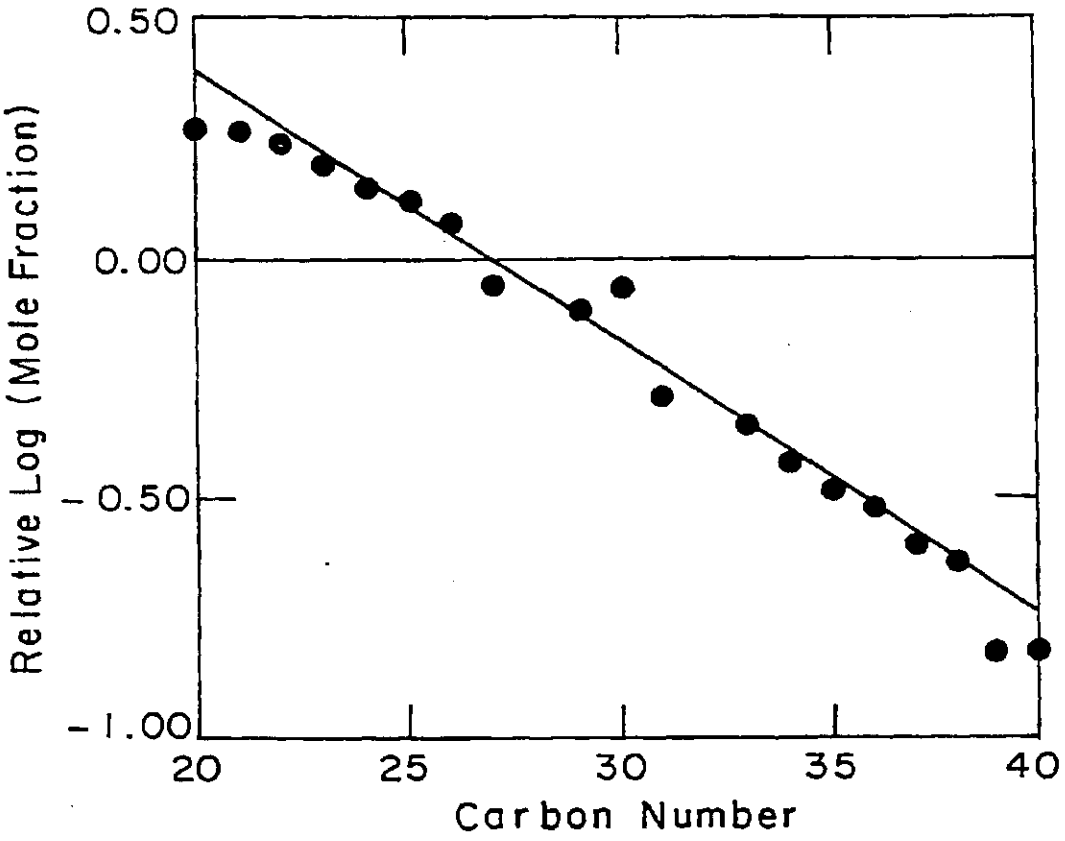

Figure 2 Schulz-Flory Distribution for Slurry Wax after 170 Hours on Stream. 260°C, 1.48 MPa, 0.022 Nl/min/gcat 1:1 H_2/CO.

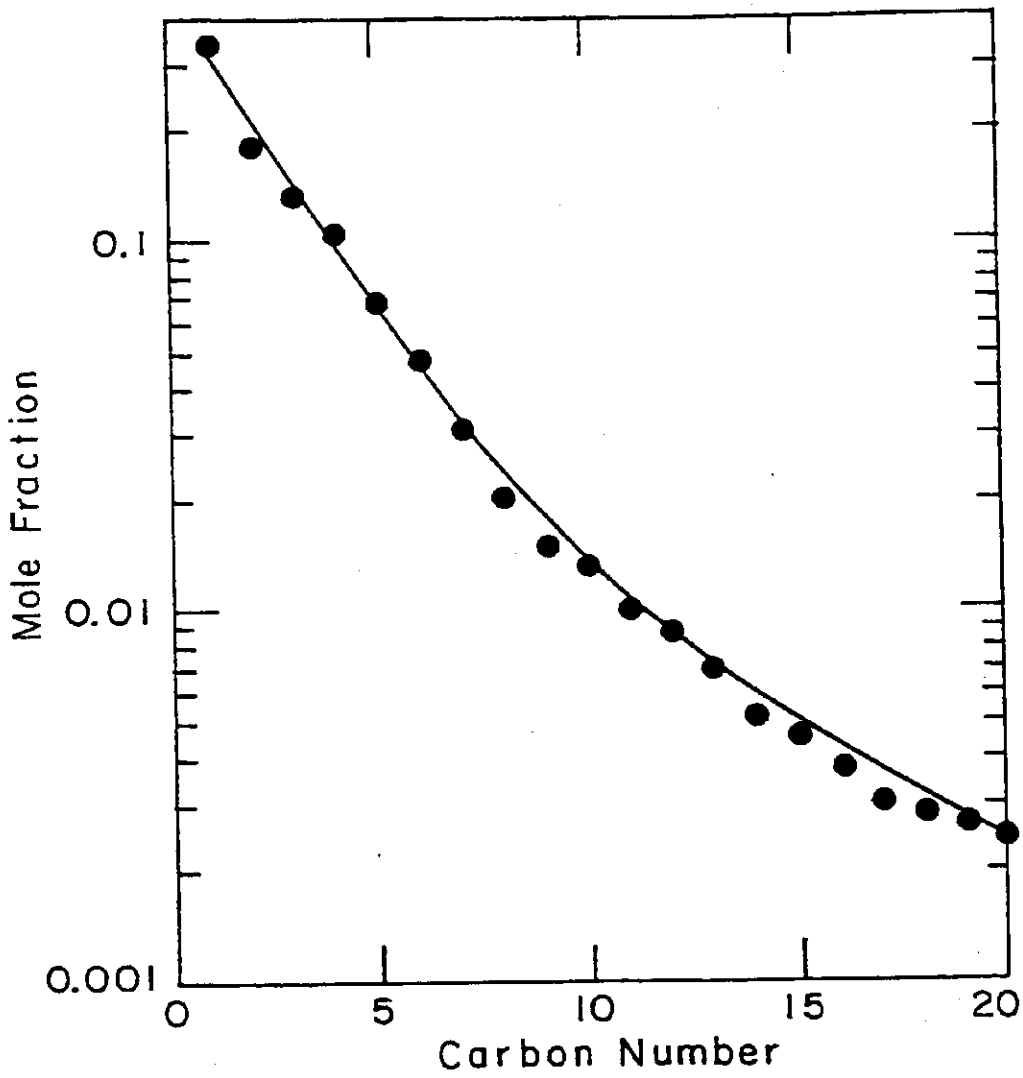

Figure 3 Schulz-Flory Diagram at 665 Hours on Stream. 260°C, 1.48 MPa, 0.022 Nl/min/gcat 1:1 H_2/CO.

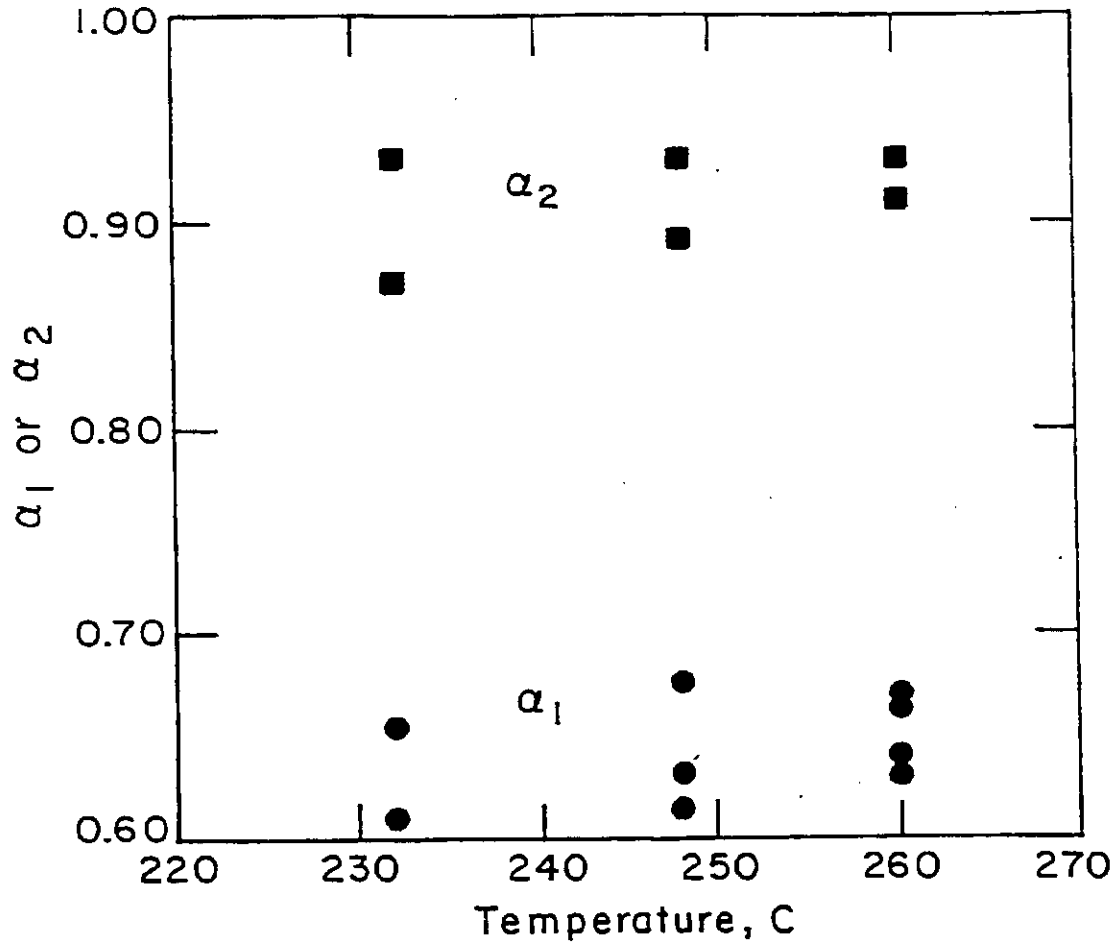

Figure 4 Temperature Dependence of α_1 and α_2.
0.022 Nl/min/gcat 1:1 H_2/CO.

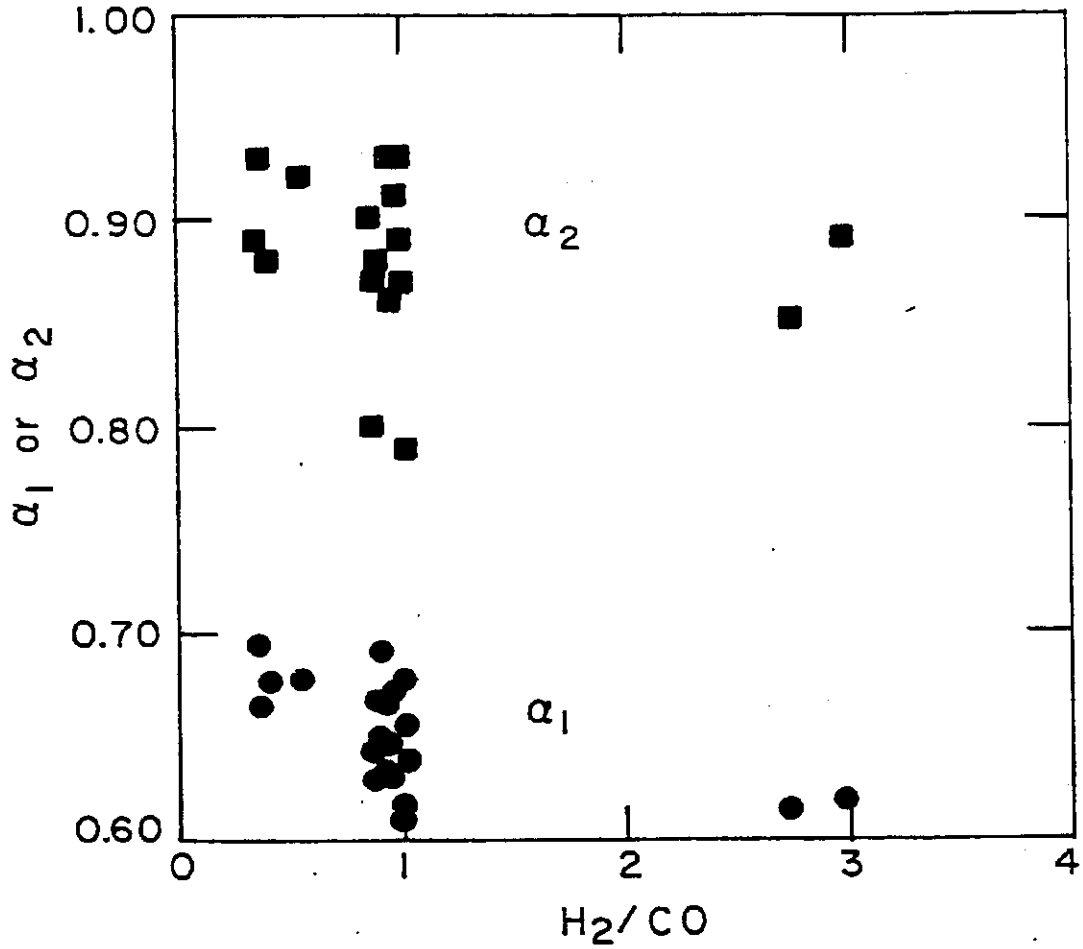

Figure 5 H_2/CO Dependence of α_1 and α_2. 260°C.

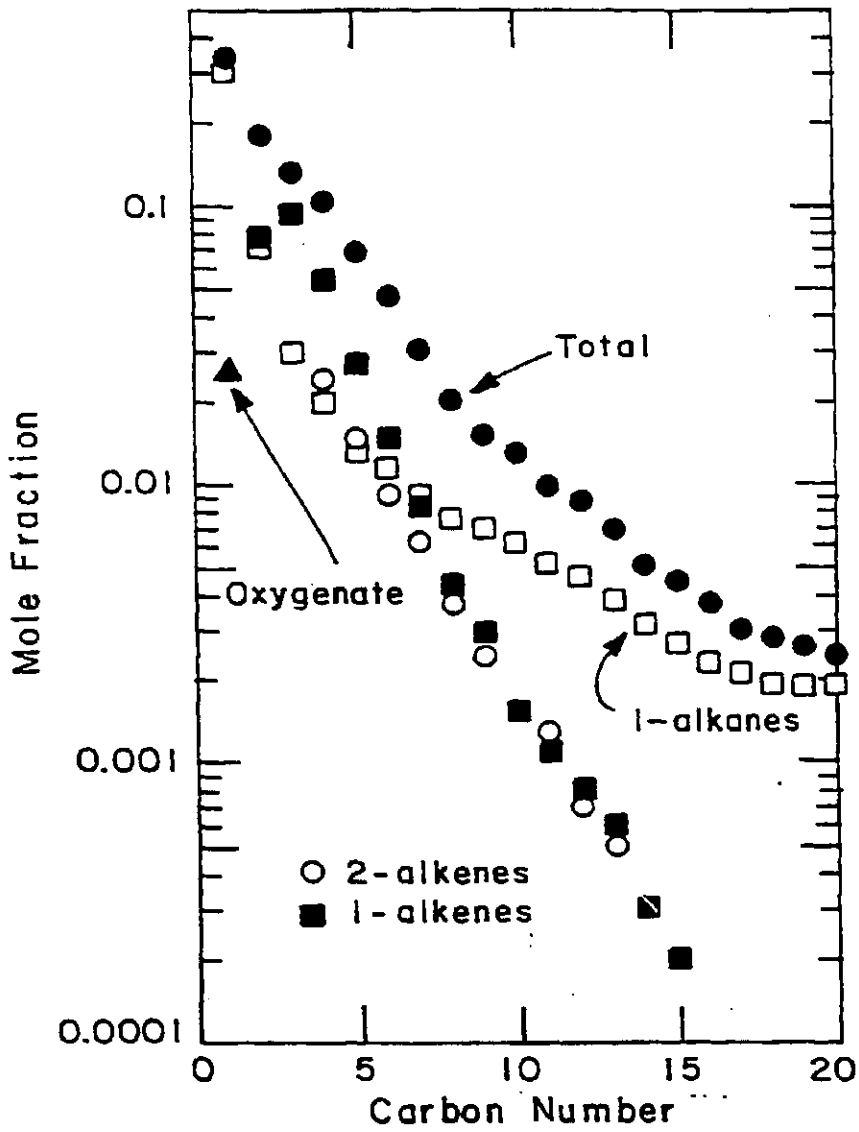

Figure 6 Component Schulz-Flory Diagram for Overhead Products at 665 Hours on Stream. 260°C, 1.48 MPa, 0.022 Nl/min/gcat 1:1 H_2/CO.

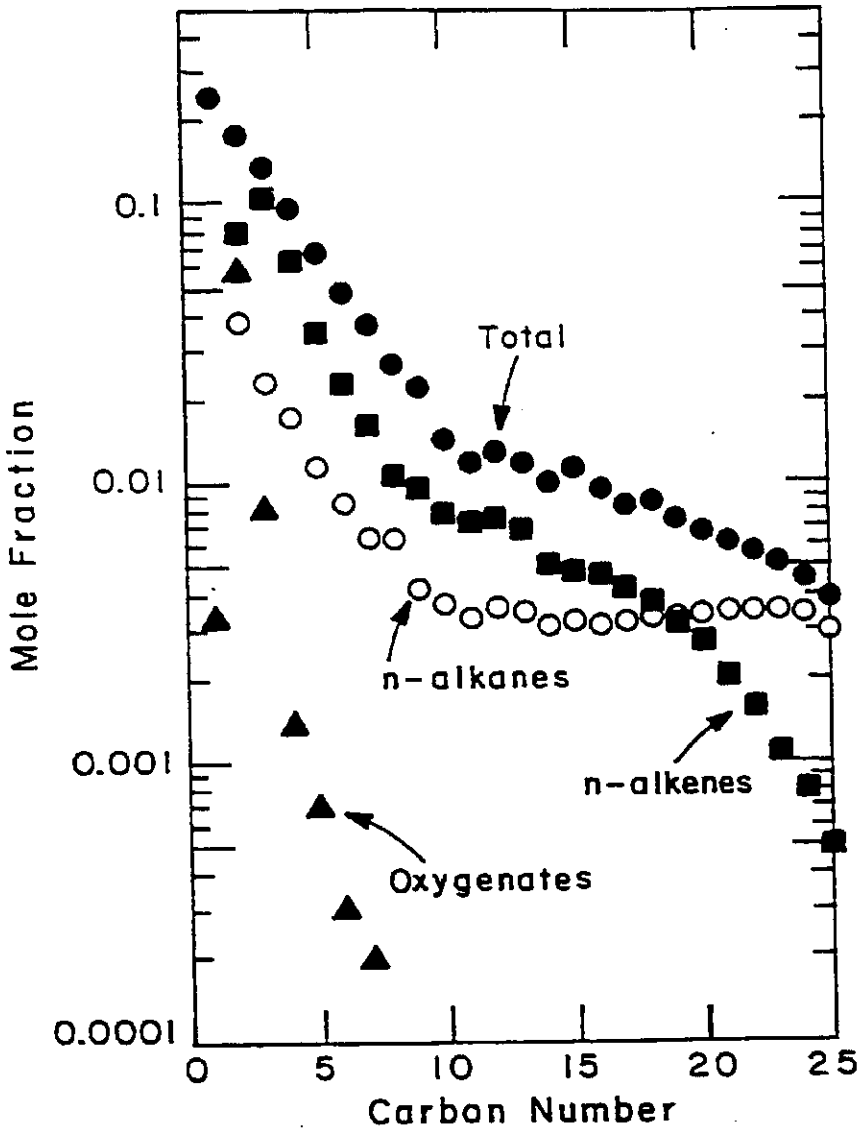

Figure 7 Component Schulz-Flory Diagram for Overhead Products at 1400 Hours on Stream, after Potassium Addition. 260°C, 1.48 MPa, 0.022 Nl/min/gcat 1:1 H_2/CO.

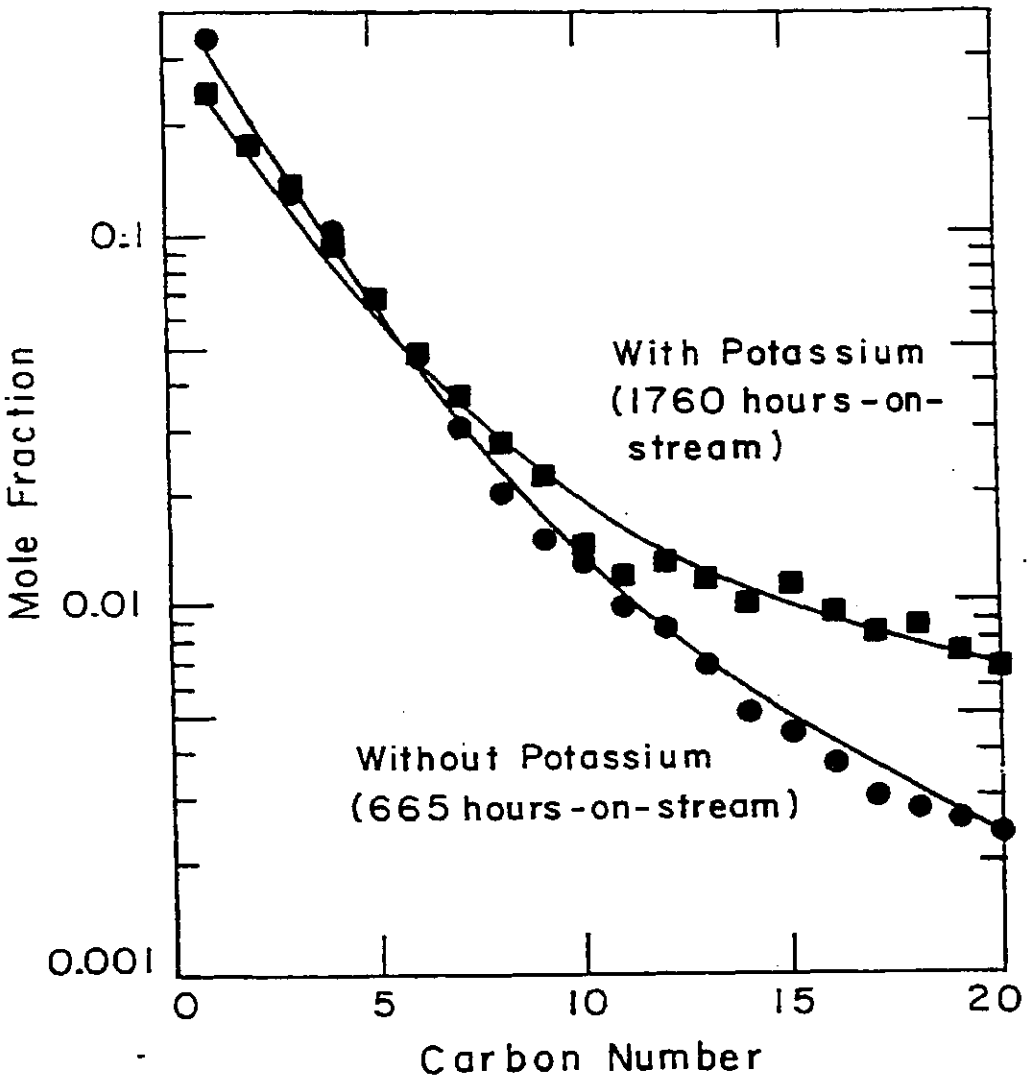

Figure 8 Effect of Potassium Addition on Schulz-Flory Diastribution of Overhead Products. 260°C, 1.48 MPa, 0.022 Nl/min/gcat 1:1 H_2/CO.

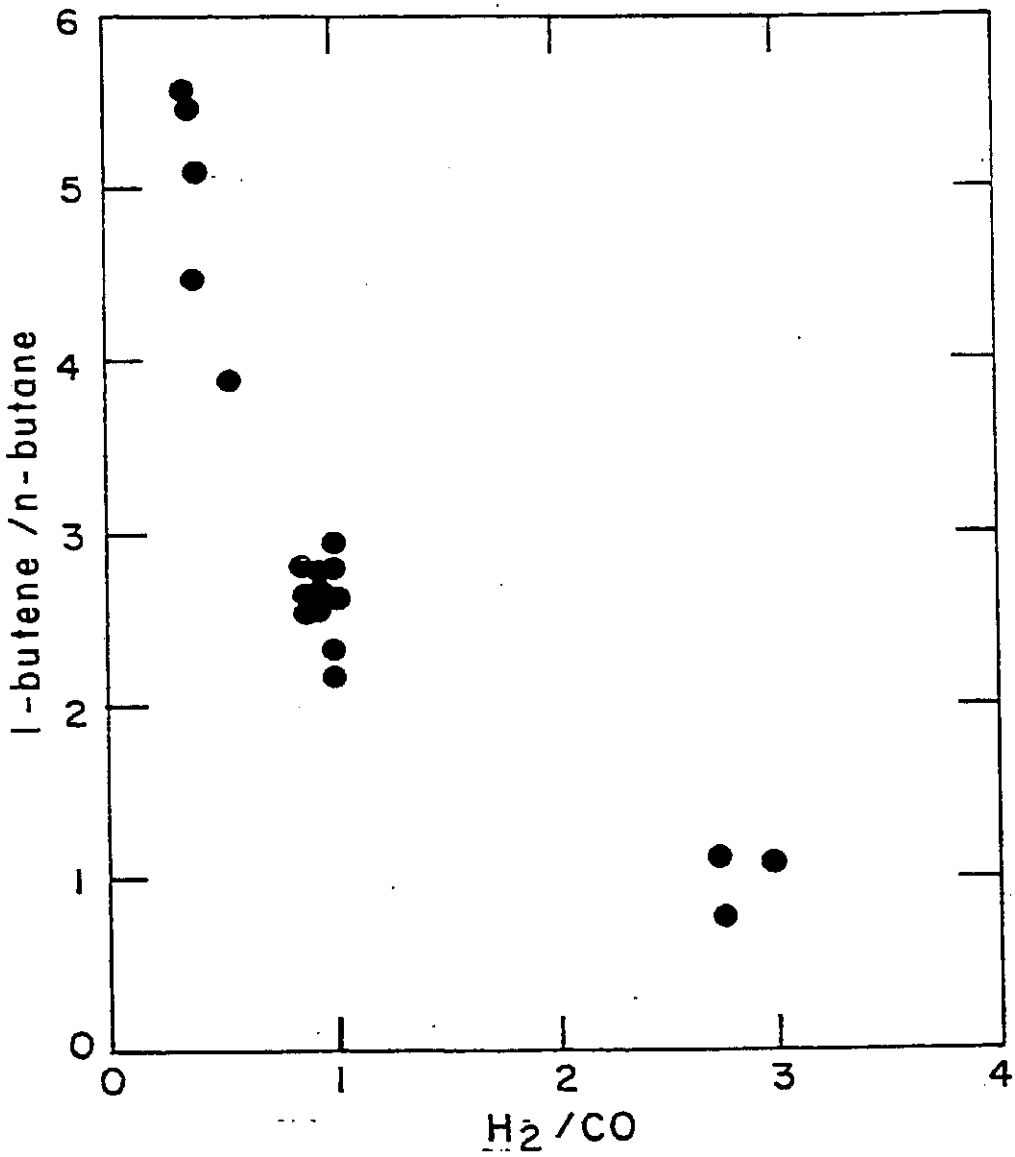

Figure 9 Ratio of 1-butene/n-butane decreases with H_2/CO Ratio in Reactor. 260°C.

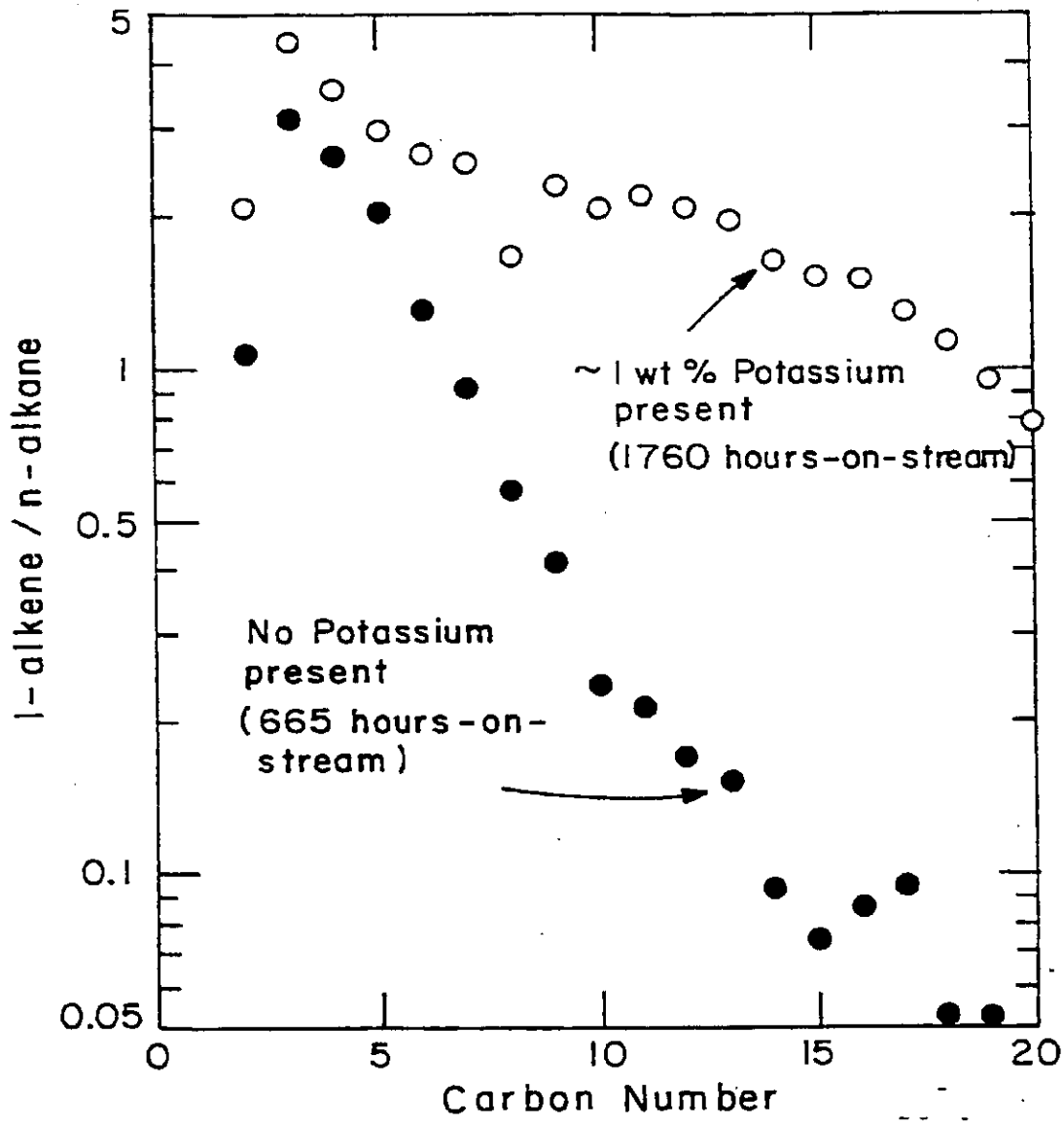

Figure 10 Ratio of 1-alkene/n-alkane Decreases With Carbon Number. 260oC, 1.48 MPa, 0.022 Nl/min/gcat 1:1 H_2/CO.

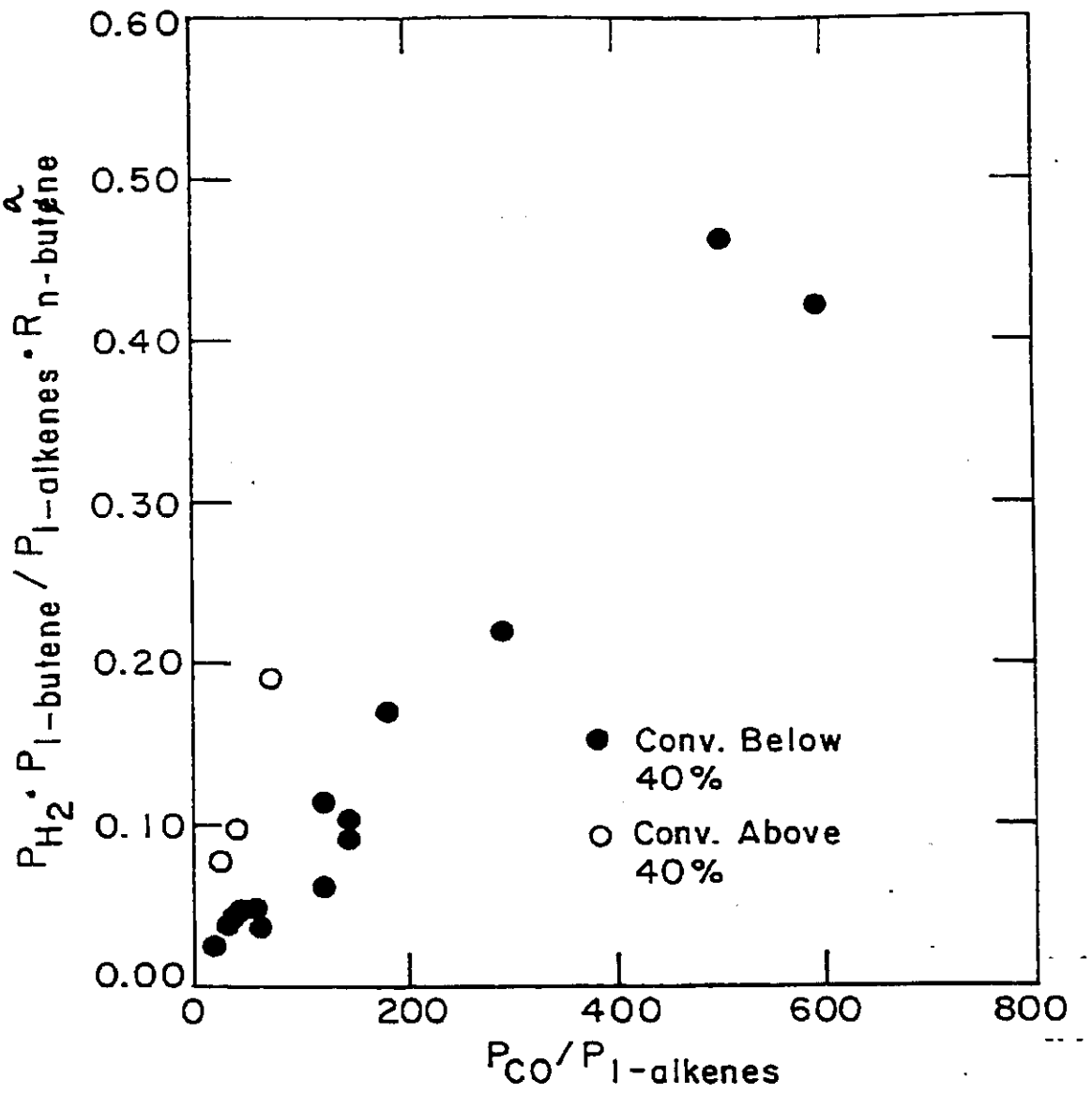

Figure 11 Model for 1-butene Hydrogenation with Inhibition by CO and 1-alkenes. 260°C.

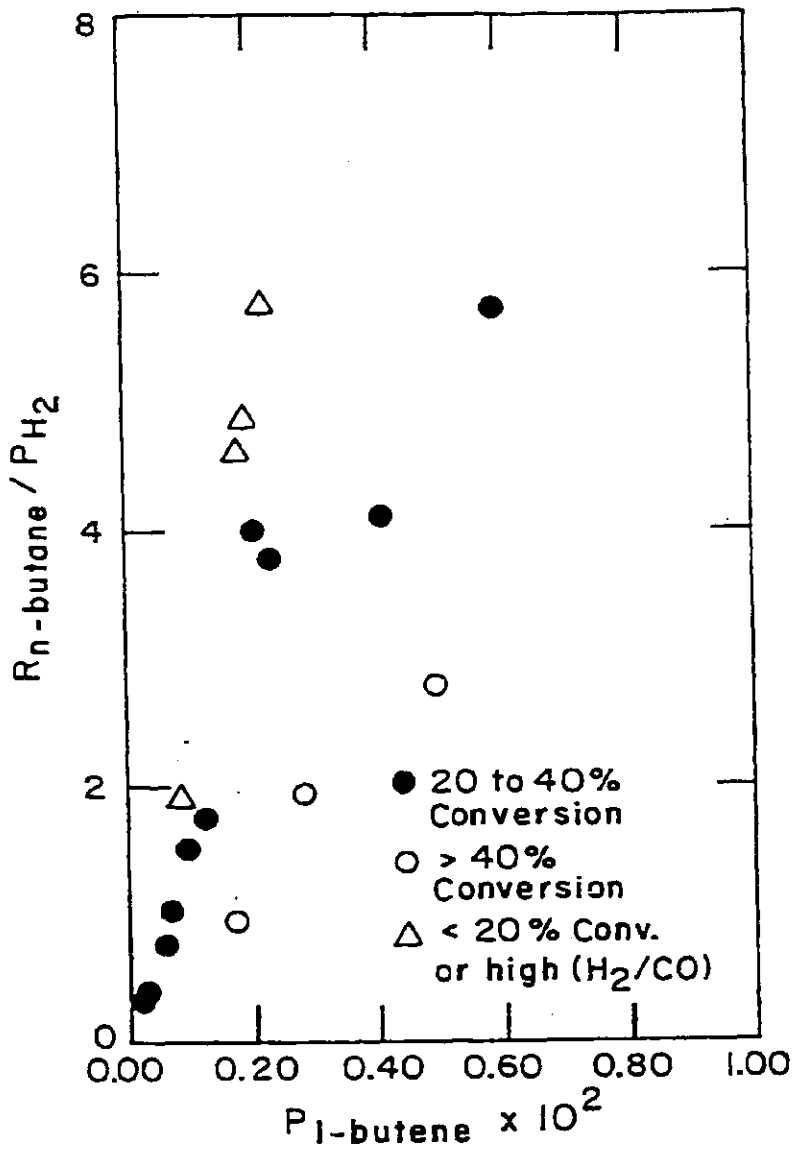

Figure 12 Dependence of n-butane Production on 1-butene Pressure. 260°C.

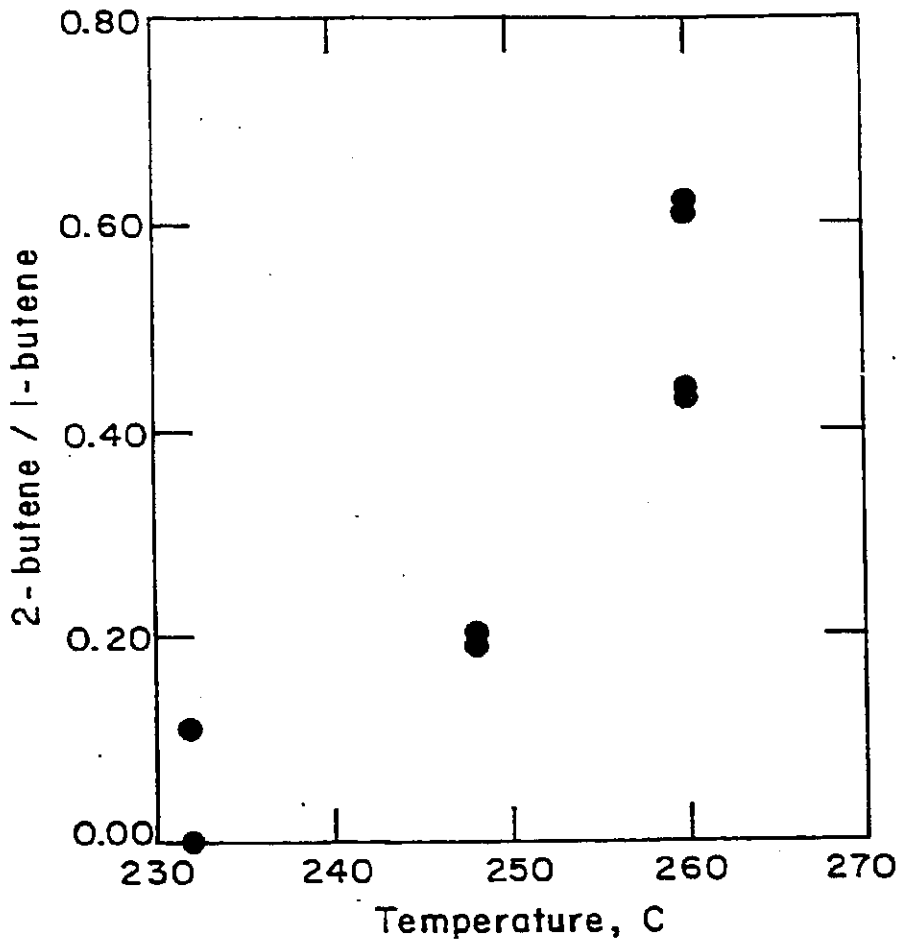

Figure 13 Ratio of 2-butene/1-butene Increases with Temperature. 0.022 Nl/min/gcat 1:1 H_2/CO.

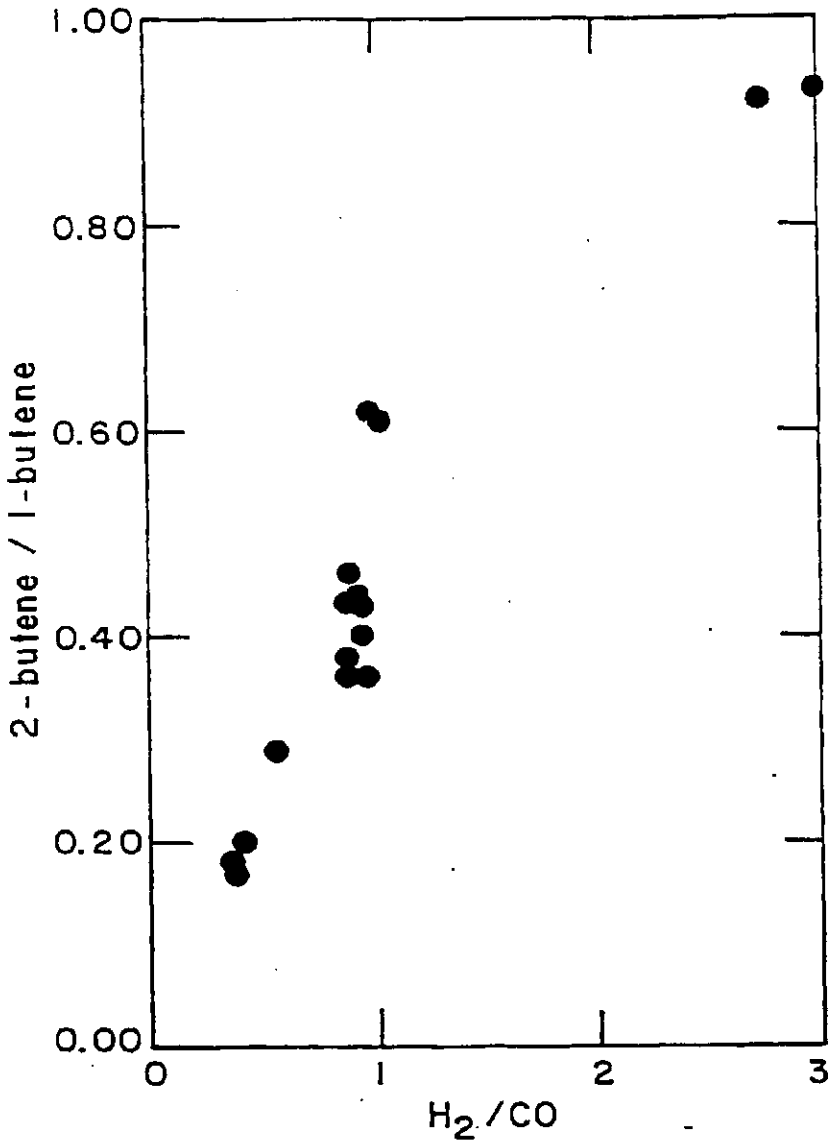

Figure 14 Ratio of 2-butene/1-butene Increases with H_2/CO Ratio in Reactor. 260°C.

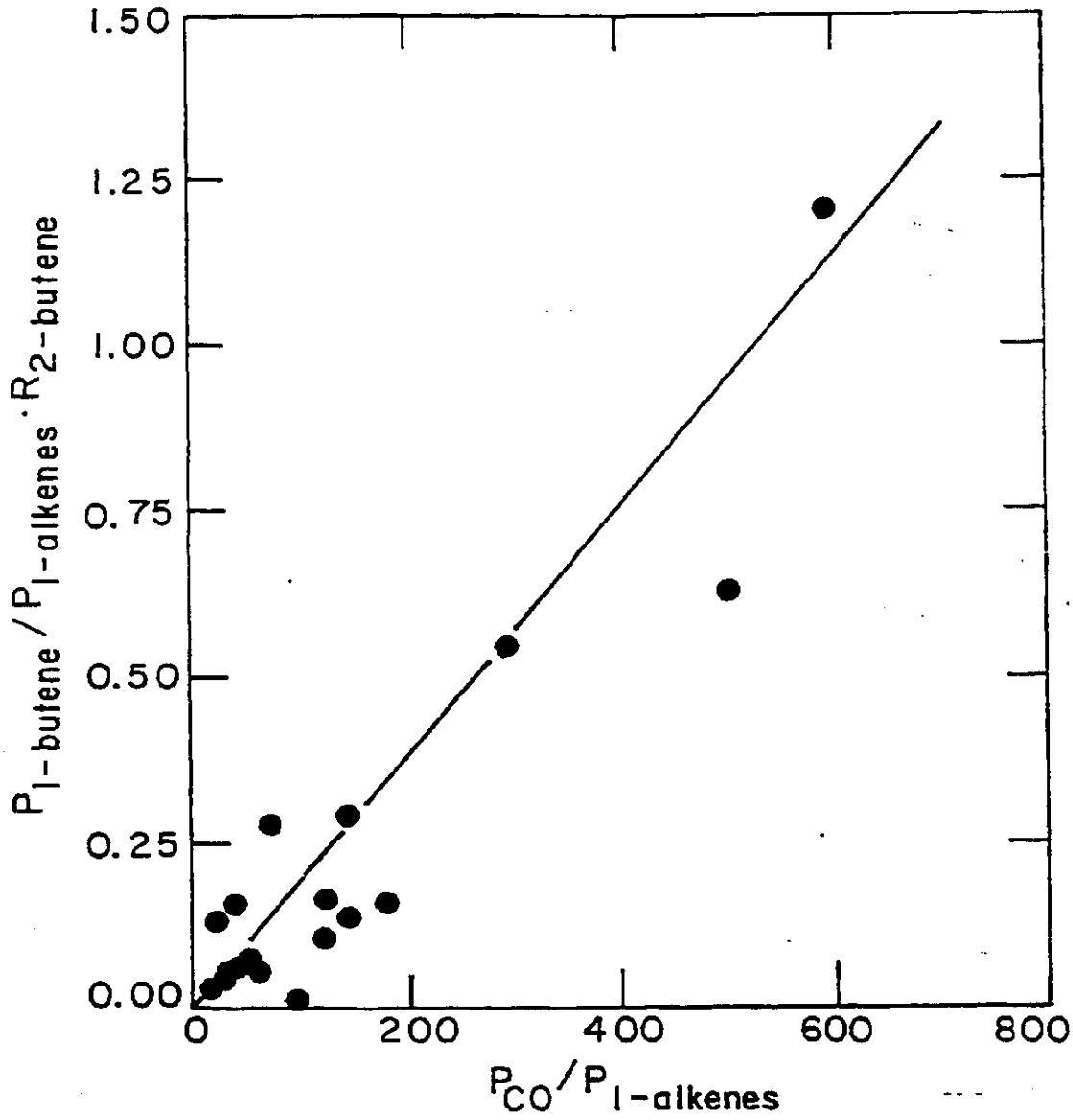

Figure 15 Model for 1-butene Isomerization with Inhibition by CO and 1-alkenes. 260°C.

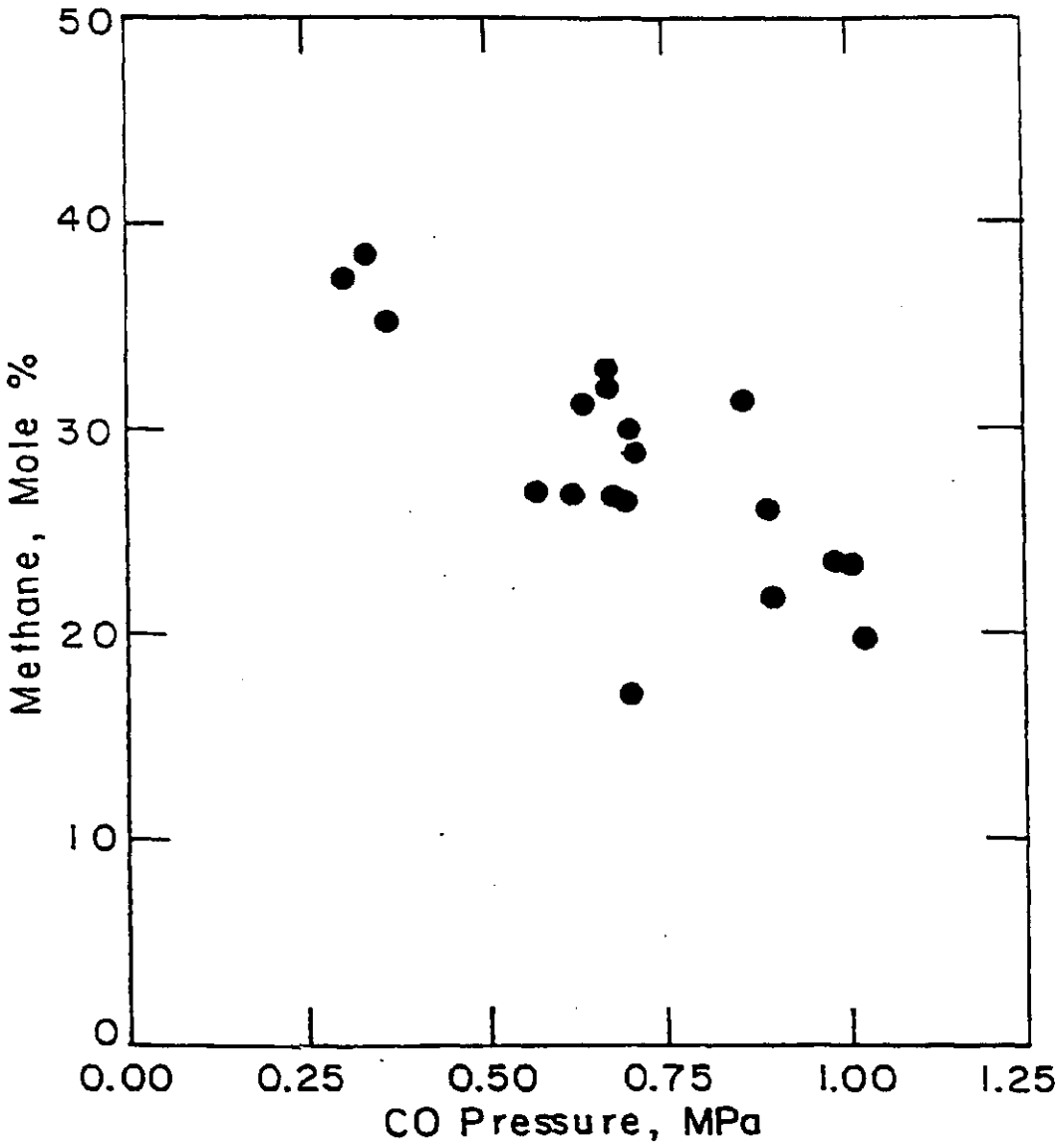

Figure 16 Mole Fraction Methane in Products Decreases with Increased CO Pressure. 260C.

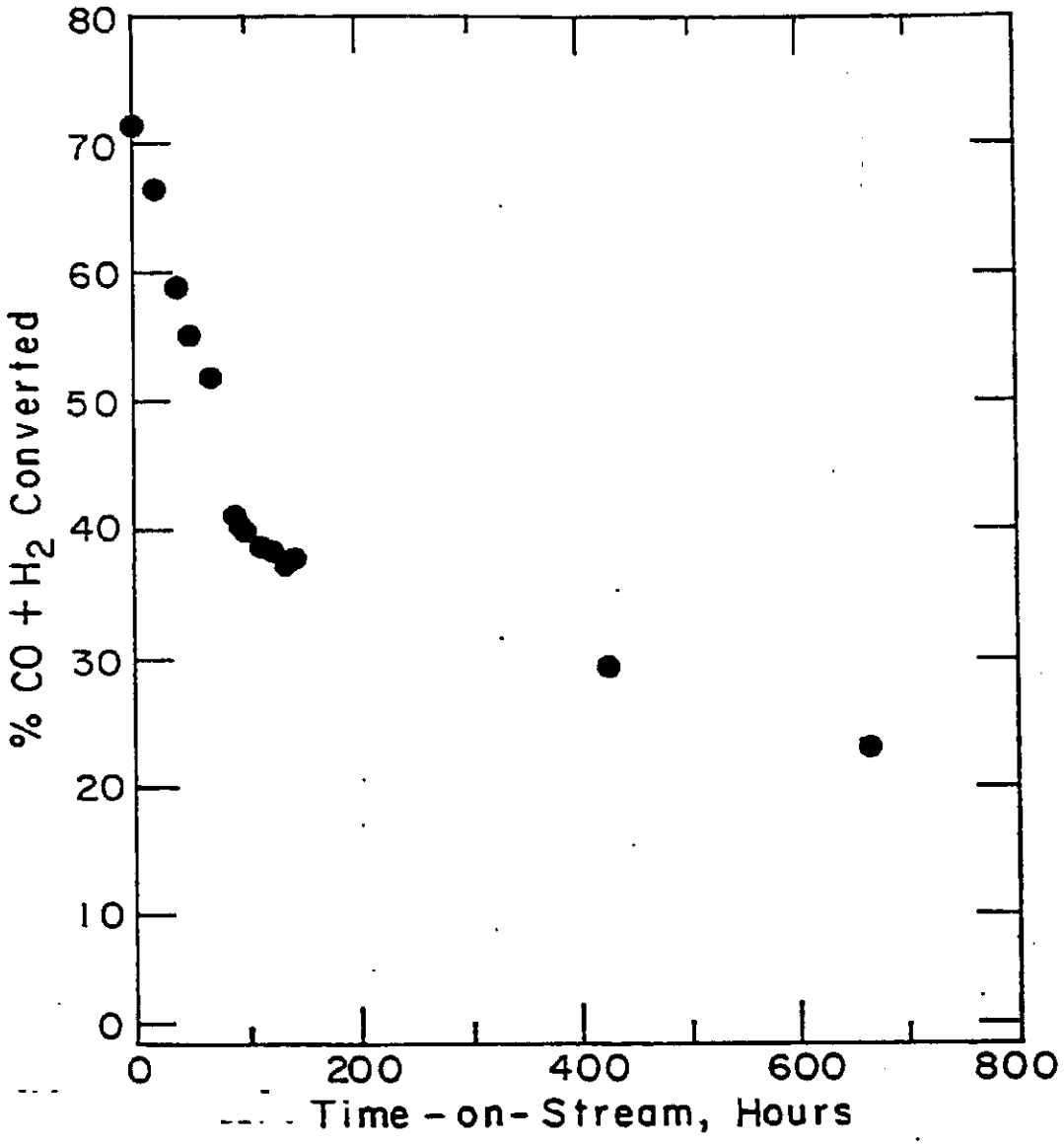

Figure 17 Deactivation of Catalyst Through 800 Hours on Stream. 260°C, 1.48 MPa, 0.022 Nl/min/gcat 1:1 H_2/CO.